이학석사학위논문

Characterization of a Multiple Branching Mutant of Arabidopsis Isolated by Activation Tagging Mutagenesis

애기장대에서 활성화 표지 돌연변이법을 통해 선별된 다지형 돌연변이 특성 분석

2013년 2월

서울대학교 대학원

생명과학부

요 정 이

JINGYI YAO

ABSTRACT

Characterization of a Multiple Branching Mutant of Arabidopsis Isolated by Activation Tagging Mutagenesis

Jingyi Yao

School of Biological Sciences

The Graduate School

Seoul National University

The *ATL98246* mutant plant that showed a multiple branching phenotype was isolated from activation tagging lines of *Arabidopsis* Columbia ecotype (Col-0). The *ATL98246* mutant plant exhibited reduced apical dominance and bushy dwarf phenotypes in the long day condition. The expression of the *At5g19700* gene was increased by the *CaMV 35S* enhancer in the *ATL98246* mutant plant. Recapitulation analysis by ectopic expression of the *At5g19700* gene under the *CaMV 35S* promoter identified that the *At5g19700* gene was responsible for the multiple branching phenotype of the *ATL98246* mutant plant. The *At5g19700* gene encodes a member of the MATE transporter protein family. The *At5g19700::GFP* fusion

protein was located in the vacuolar membrane. RT-PCR analysis with different tissues of the wild type plants suggested that the *At5g19700* gene was expressed in the leaves, roots, stems, floral clusters, and siliques. The expression levels of some IAA (Indole-3-Acetic Acid) inducible genes in different tissues, for example *IAA5*, *IAA6* and *IAA19* genes, were changed in the *ATL98246* mutant plant, which may suggest that auxin be involved in the multiple branching phenotype in the *ATL98246* mutant plant.

Keywords: Shoot branching, MATE transporters, Activation tagging mutagenesis, *Arabidopsis*

Student Number: 2010-24007

CONTENTS

ABSTRACT……2

CONTENTS……4

LIST OF FIGURES……5

LIST OF TABLE……6

LIST OF ABBREVIATION……...……...……..7

INTRODUCTION……...……8

MATERIALS AND METHODS……...……20

RESULTS……..……29

1. The phenotypes with the *ATL98246* mutant plant was phenocopied in the recapitulation plant……..……..29

2. The At5g19700 protein is a member of the MATE protein family……...31

3. The *At5g19700* gene is expressed in the whole plant and strongly expressed in siliques 38

4. The subcellular localization of At5g19700 protein is on the vacuolar membrane……42

5. Characterization of the T-DNA insertional *CS878754* mutant plant……44

6. The alternation of the expression level of *IAA* genes in th*e ATL98246* mutant plant…...46

DISSCUSSION……51

REFERENCES……..……55

국문 초록……..……61

ACKNOWLEDGEMENT……62

LIST OF FIGURES

Figure 1. The phenotypic comparison between wild type and the *ATL98246* mutant plants

Figure 2. The T-DNA insertion site and expression level of T-DNA adjacent genes in the *ATL98246* mutant plant

Figure 3. The multiple branching phenotype was rescued in the recapitulated plant

Figure 4. The phylogenetic tree of 56 members in the MATE superfamily

Figure 5. The multiple sequence alignment of the At5g19700 protein with other eight MATE proteins

Figure 6. The potential transmembrane motifs and hydrophobic plot prediction of the At5g19700 MATE protein

Figure 7. The expression pattern of the *At5g19700* gene in *Arabidopsis*

Figure 8. The subcellular localization of the At5g19700 protein

Figure 9. The T-DNA insertion site, expression level of *At5g19700* gene and phenotypic comparison between wild type and the T-DNA insertional *CS878754* mutant plants

Figure 10. The RT-PCR analysis of the auxin-inducible genes in wild type, *ATL98246* mutant and *CS878754* mutant plants

LIST OF TABLE

Table 1. List of primer sequences used in this study

LIST OF ABBREVIATION

CaMV 35	Cauliflower mosaic virus 35S
cDNA	Complementary DNA
CTAB	Cetyl trimethylammonium cromide
EDTA	Ethylenediaminetetraacetic acid
GUS	Glucuronidase
IAA	Indole-3-acetic acid
LB	Luria-Bertani
MATE	Multidrug and toxic compound extrusion protein
PCR	Polymerase chain reaction
PVP	Polyviny-polypyrrolidone
rpm	Revolution per minute
RT-PCR	Reverse transcription polymerase chain reaction
TE	Tris and EDTA
Tris	Tris(hydroxymethyl) aminomethane
X-GlcA	5-bromo-4-chloro-3-indolyl-β-D-glucuronic acid

INTRODUCTION

The regulation of shoot architecture is important for plant adaptation, survival, and competition (Ferguson *et al.,* 2009). Shoot branching is the process that a dormant bud activates, develops and turns into branch. In plant, the basic apical–basal axis is formed during embryonic development. The shoot apical meristem is established at the apex and the root apical meristem is established at the basal end. The formation of shoot-specific organs is defined by the activity of shoot apical meristem. The classical hypothesis of apical dominance suggests that the shoot apex inhibits the outgrowth of lateral buds, and is critical for the shoot architecture regulation (Ongaro *et al.*, 2008). Actually, each secondary meristem has the same development potential as the primary shoot apical meristem (SAM) to grow out to produce a branch, thus a secondary shoot can arise through the activation of the axillary meristem. The axillary meristem often initiates a few leaves before arresting their growth to form a dormant axillary bud. This bud may be activated and given rise to a branch later or may remain dormant. Thus, the final number of branches is defined by the number of axillary meristems and by the activity of the axillary buds (Domagalska *et al.,* 2011). The formation of axillary meristems and the subsequent regulation of their activity contribute greatly to variation in shoot architecture (Bennett *et al.,* 2006; Müller *et al.,* 2011).

The regulation of bud outgrowth is affected by both internal and environmental signals. The specialized regulation system of a variety of molecule signals

processes on the shoot architecture development. Three classes of hormones auxin, cytokinins (CKs) and strigolactones (SLs) move throughout the plant forming a network of systemic signals to control the shoot branching in *Arabidopsis*.

Auxin, as an inhibitory substance, is produced in the apex and young expanding leaves, moves basipetally and inhibits the bud outgrowth indirectly because auxin does not enter the bud. Cytokinins (CKs) is mostly synthesized in both shoot and root, and transported acropetally in the xylem as a bud outgrowth activator. Unlike auxin, CKs directly promotes bud growth. It has been reported that auxin reduces CK synthesis through repressing the *adenosine phosphate-isopentenyltransferase (IPT)* gene encoding a CK biosynthetic enzyme expression depending on Auxin Resistant1 (AXR1)-mediated auxin signaling (Nordström *et al.,* 2004). Another branch inhibitor strigolactones (SLs), which are also synthesized in shoot and root, are transported acropetally to repress bud activity (Domagalska *et al.,* 2011). The function of SL-related genes is characterized best in *Arabidopsis* where three of four *MORE AXILLARY BRANCHES (MAX)* genes (*MAX1*, *MAX3*, and *MAX4*) have been suggested to be involved in the biosynthesis of SLs (Agustia *et al.,* 2011). The *MAX3* and *MAX4* genes encode plastid-targeted carotenoid cleavage dioxygenases (CCDs), together with the cytochrome P450 family member MAX1 protein, to control the production of upwardly mobile signal (SL) that inhibits axillary bud outgrowth (Hayward *et al.,* 2009). In the shoot, SL signal transduction probably involves MAX2 protein which is the F-box leucine-rich repeat protein that acts as a component of the SCF-like protein ubiquitin ligase complex to target specific

proteins for ubiquitylation.

There are two generally accepted hypotheses for the dormant bud activation: the auxin transport canalization-based model and second messenger model. The auxin transport canalization-based model suggests that the primary shoot apex and the secondary axillary buds are the potential auxin sources. Apical dominance is determined directly by the flow of auxin in the plant. Auxin is transported from the main shoot apex impeding the flow of auxin from the bud to prevent the bud outgrowth. According to this theory, no matter the apical shoot or the axillary buds, only the one can grow when it actively exports auxin basipetally (Ferguson *et al.*, 2009). Auxin is transported from the axillary buds into the main stem basipetally to root and this auxin flux establishes the polar auxin transport (PAT) stream. For the primary axillary bud, auxin is exported to the main stem when high level flux occurs, which will trigger the activation of this axillary bud. In the meanwhile, this high level auxin flux in the main stem exporting from the activated bud prevents the additional auxin exporting from other buds to reduce the flux (low flux). Therefore, these secondary axillary buds will remain dormant because of the low auxin flux.

The other hypothesis of the hormone controlled branching is the second messenger model depending on the auxin signaling pathway. Auxin up-regulates SL to inhibit the bud outgrowth while down regulating the CKs to promote bud outgrowth. In the stem, auxin induces the production of the second messenger SL by up-regulating the expression level of the SL synthetic genes *MAX3* and *MAX4*

and reduces CK level by regulating the transcription level of the *ADENYLATE ISOPENTENYLTRANSFERASE (IPT*) family genes, which have a key role in the CKs biosynthesis (Tanaka *et al.*, 2006).

Nowadays, many multiple branching mutants and the branching related genes have been studied by researchers.

transparent testa (*tt4*) plant was a mutation in the gene encoding the first enzyme in flavonoid biosynthesis, chalcone synthase. *tt4* mutant showed three times as many secondary inflorescence stems, reduced plant height, and decreased stem diameter. Auxin transport is elevated in plants with a *tt4* mutation. In hypocotyls of *tt4*, this elevated transport is reversed when flavonoids are synthesized by growth of plants on the flavonoid precursor, naringenin (Brown, *et al.*, 2001). *iaa28-1* is an auxin-resistane mutant that has diminished adult size, decreased apical dominance and defective in lateral root formation. *IAA28* transcription is not induced by exogenous auxin. IAA28 normally represses transcription, perhaps of genes in response to auxin signals (Rogg, *et al.*, 2001).

The activation tagging mutant *ATL98246* with abnormal morphological phenotypes studied here was screened from an activation-tagging mutant pool that was generated by transforming Col-0 plants with the activation-tagging vector pSKI015. This activation tagging vector has a T-DNA with four copies of enhancer elements from a *constitutively active cauliflower mosaic virus (CaMV) 35S* gene, pUC19 sequences with a bacterial origin of replication and an ampicillin resistance gene for plasmid rescue, glufosinate resistance (BAR) sequences for making the

mutant survive from Basta selection (Odell *et al.*, 1985), left border and right border. The *CaMV 35S* enhancers, which are at the right border, can cause nearby genes' transcriptional activation to form a gain-of-function mutation that the phenotype could be observed in T1 generation. Furthermore, the *CaMV 35S* enhancers primarily enhanced an endogenous expression pattern and do not induced constitutive ectopic expression (Weigel *et al.*, 2000; Ahn *et al.*, 2007).

The *ATL98246* mutant plant exhibited fast-growth, bushy dwarf and reduced apical dominance with multiple branching phenotypes in the long day condition. In the 2 week old stage, the plant body and leaves of *ATL98246* mutant were smaller than those of wild type plant (Figure 1A and D) and the *ATL98246* mutant plant started branching from 2 week old, which was earlier than wild type plant (Figure 1B). The *ATL98246* mutant plant showed shorter siliques than those of will type plant (Figure 1E). In the 7 week old plant, both the number of rosette-leaf branches (the inflorescences that developed from rosette leaves) and cauline-leaf branches (the inflorescences that developed from cauline leaves) were increased and the height of the plant was reduced in the *ATL98246* mutant plant (Figure 1C). Figure 1F shows the branch development of *Arabidopsis* and the schematic diagrams of the different branch development model of wild type and *ATL98246* mutant plants (Figure 1G). The number of rosette-leaf branches and cauline-leaf branches on the primary shoot of wild type plant were ranged from 2 to 3. In the *ATL98246* mutant plant, the number of rosette-leaf branches and cauline-leaf branches on the primary shoot were at the range of 5 or 6, and the secondary cauline-leaf branches

continued to produce from axils of cauline leaves (Figure 1G, H and I). The total branch number increased to 100 in the homozygous *ATL98246* mutant plant (Figure 1J).

The T-DNA insertion site of the *ATL98246* mutant was confirmed and the homozygous and heterozygous plants were figured out by genotyping PCR (Figure 2B). Unlike other activation tagging mutants, in the *ATL98246* mutant plant an extra 1.7 kb fragment from left border of T-DNA was integrated into the plant genome, identified by the sequencing result of the genotyping PCR product. Among the F2 generation produced by self-fertilization of the heterozygous F1 plants, approximately 25% of F2 plants exhibiting wild-type phenotype were herbicide-susceptible. 75% retained the mutant phenotypes and were herbicide resistant, among which 25% were homozygous plants confirmed by genotyping PCR. The segregation ratio of F2 generation by genotyping PCR results was 1:2:1.

RT-PCR analysis was carried out to detect the transcription levels of the three genes (*At5g19700, At5g19710* and *At5g19720*) nearby the T-DNA insertion site with their specific primer sets, respectively. The transcription level of the *At5g19700* gene was increased in the *ATL98246* mutant plant. The *At5g19710* gene was expressed lower degree in the *ATL98246* mutant than that of the wild type plant resulting from the inserted T-DNA in the *At5g19710* gene. Transcription level of the *At5g19720* gene was equal between the *ATL98246* mutant and wild type plants (Figure 2C).

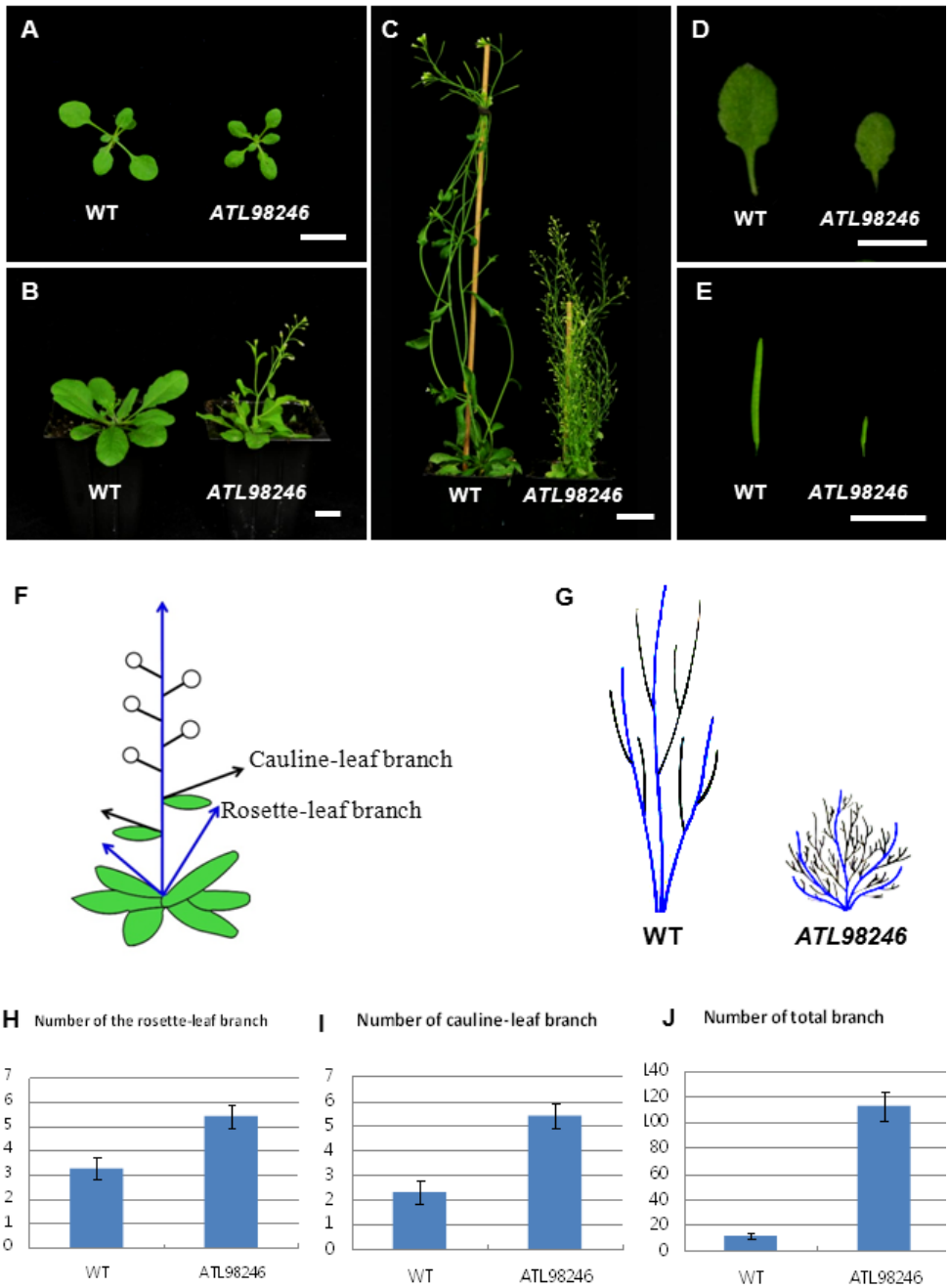

Figure 1. The phenotypic comparison between wild type and the *ATL98246* mutant plants

(A) View of 2 week old plants grown under the long day condition on soil. From

left to right: wild type and *ATL98246* mutant plants. Scale bar: 1 cm.

(B) View of 3 week old plants grown under the long day condition on soil. From left to right: wild type and *ATL98246* mutant plants. Scale bar: 1 cm.

(C) View of 7 week old plants grown under the long day condition on soil. From left to right: wild type and *ATL98246* mutant plants. Scale bar: 1 cm.

(D) Comparison of rosette leaves. Plants were grown under the long day condition on soil. From left to right: wild type and *ATL98246* mutant plants. Scale bar: 1 cm.

(E) Phenotypes of 7 week old siliques grown under the long day condition. From left to right: wild type and *ATL98246* mutant plants. Scale bar: 1 cm.

(F) Model of the branch structure of *Arabidopsis*. Blue arrows present rosette-leaf branches; black arrows present cauline-leaf branches; circles present floral clusters; green ellipses present leaves.

(G) The schematic diagrams of the different branch development model of wild type and *ATL98246* mutant plants. Blue lines present rosette-leaf branches; black lines present cauline-leaf branches.

(H) The rosette-leaf branch number of wild type and *ATL98246* mutant plants.

(I) The cauline-leaf branch number on the primary shoot (rosette-leaf branch) of wild type and *ATL98246* mutant plants.

(J) The total branch number including rosette-leaf branches and cauline-leaf branches of wild type and *ATL98246* mutant plants.

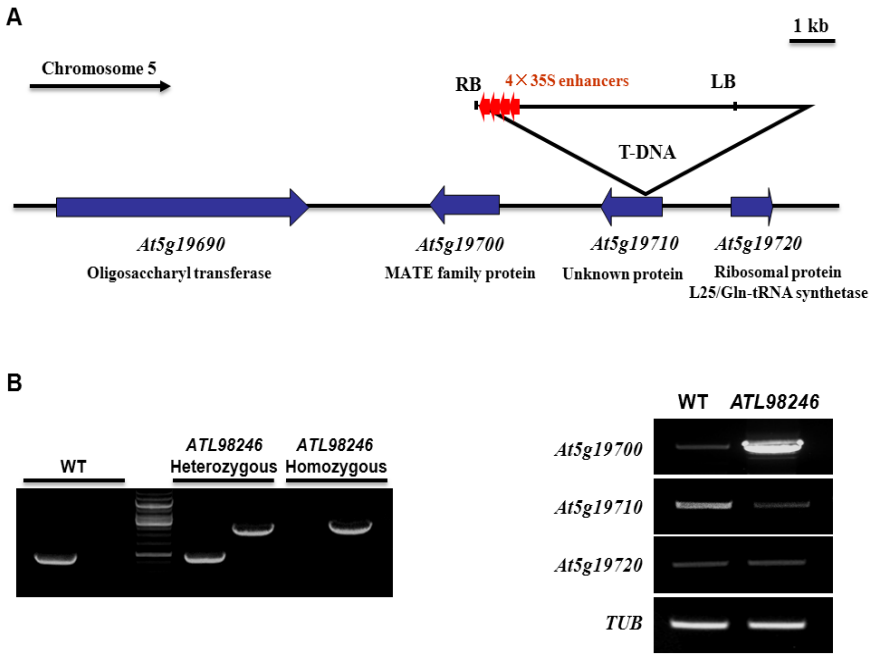

Figure 2. The T-DNA insertion site and expression level of T-DNA adjacent genes in the *ATL98246* mutant plant

(A) The T-DNA insertion site of the *ATL98246* mutant plant. Four arrows show the *35S* enhancer at the right border of the T-DNA. The description of the genes is from TARI database. Scale bar: 1 kb DNA length.

(B) Confirmation of the T-DNA insertion site with heterozygous and homozygous *ATL98246* mutant plants by genotyping PCR analysis.

(C) RT-PCR analysis of the expression levels of *At5g19700*, *At5g19710* and *At5g19720* genes that located nearby the T-DNA insertion site. RNA isolated from 4 week old whole plants was used for the RT-PCR analysis.

The *Tubulin* gene was used for normalization.

The *At5g19700* gene belongs to a member of the MATE family in *Arabidopsis*. Multidrug and toxic compound extrusion (MATE) is a family of transporter proteins, which widely distributed in all living kingdoms (Burko *et al.*, 2011). Although the length of proteins in the MATE family ranges from 400 to 700 amino acids, most members consist of 400-500 residues with 10 to 12 transmembrane helices (Omote *et al.*, 2006). The MATE transporter family members transport a variety of compounds: bacterial MATEs are respected to cationic drug transportation, fungal MATEs confer the resistance to methionine analog ethionine, and mammalian MATEs work as organic cation tetraethylammonium transporters. So far, the plant MATE family has large members of orthologues and family members are reported to transport secondary metabolites and xenobiotics through an H^+ exchange mechanism (Omote *et al.*, 2006; Moriyama *et al.*, 2008). The ABERRANT LATERAL ROOT FORMATION5 (ALF5/At3g23560) protein is required for protection of roots from inhibitory compounds like the tested toxic cation, tetramethylammonium (Diener *et al.*, 2001). The ENHANCED DISEASE SUSEPTIBILITY5 (EDS5/At4g39030) protein might function in salicylic acid-dependent disease resistance signaling, acting as a SA transporter or a precursor required for its synthesis (Nawrath *et al.*, 2002). The FERRIC REDUCTASE DEFECTIVE3 (FRD3/At3g08040) protein acts as a proton-coupled citrate exporter, extruding citrate into the xylem or the rhizosphere for the iron homeostasis (Durrett *et al.*, 2007). The *A. thaliana* DETOXIFICATION1 (AtDTX1/At2g04040) protein is a detoxifying efflux carrier, which may be

required for the protection of the roots from naturally occurring toxic compounds (Li *et al.*, 2002). TT12 and FFT protein were identified as flavonoid transporters that related to seed development. The TRANSPARENT TESTA12 (TT12/At3g59030) protein is thought to control the sequestration of flavonoids, the anthocyanin transport to reduce the anthocyanin accumulation in the seed coat endothelium (Debeaujon *et al.*, 2001; Marinova *et al.*, 2007; Zhao *et al.*, 2009). The Flower Flavonoid Transporter (FFT/At4g25640) protein mediates flavonoid transport to affect root growth, seed development and germination, and pollen development (Thompson *et al.*, 2009; Thompson *et al.*, 2010). Some MATE genes dominant mutants were isolated by showing the multiple branching phenotype. Bush and Chlorotic Dwarf 1 (BCD1/At1g58340) protein is known as a transporter which is contributes to iron homoeostasis during stress response and senescence. The *bcd1-1D* plant exhibits stunted growth with reduced apical dominance and pale green and smaller leaves. The BCD1 transporter plays a role in sustaining iron homoeostasis by reallocating excess iron released from stress-induced cellular damage (Seo *et al.*, 2012). The *activated disease susceptibility 1-Dominant (ads1-D)* mutant plant shows multiple branching and reduced height phenotypes. The ADS1 protein functions in the establishment of plant disease resistance (Sun *et al.*, 2011). Although these mutants all appear reduced apical dominance with multiple branching and decreased height phenotypes, little is known about the functional mechanisms of these MATE transporters or other MATE members of *Arabidopsis* responsible for the shoot development and plant architecture.

In this study, recapitulation analysis confirmed that ectopic expression of the *At5g19700* gene is responsible for the multiple branching phenotype. The T-DNA insertional mutant *CS878754* plant was gained but did not show visible phenotype difference comparing with wild type plant. The At5g19700 protein belongs to the MATE transport family which has 56 orthologues in *Arabidopsis.* The expression pattern and subcellular localization of the *At5g19700* gene were studied. In additional, the change of the expression level of some auxin-inducible genes was analyzed by RT-PCR in different plant tissues.

MATERIALS AND METHODS

1. Plants materials and growth condition

All *Arabidopsis thaliana* plants used in this study were in the Columbia (Col-0) background. All of the mutants and Col-0 were grown in a controlled culture room at 22°C with a relative humidity of 55% under long-day conditions (16 hours of light and 8 hours of darkness) with white light illumination. *Arabidopsis* seeds were sown on the surface of soil mixed with vermiculite in small pots.

In addition, some seeds were sown on Murashige and Skoog (MS) medium. Seeds were surface sterilized in a micro centrifuge tube with 1ml 70% ethanol containing 0.06% TritonX-100 for 3 min, followed by washing three times with 100% ethanol. The seeds were dried on Whattman filter paper naturally and plated on solidified MS agar plates. These plates contained 0.5× Murashige and Skoog salts (DUCHEFA) and 0.8% (w/v) or 1.5% (w/v) plant agar (DUCHEFA, pH 5.6-5.8). The samples were transferred into the culture room after a 3 days cold treatment in 4°C refrigerator for uniform germination.

2. Bacterial strains and plasmids

Bacterial strains used in this study were *Escherichia coli* (*DH5α*) and *Agrobacterium tumefaciens* (*GV3101*) for cloning and gene transformation into wild type plants, respectively. The transformed *E. coli* containing the cloned

plasmid were cultured in the liquid LB medium (MERCK) or on solidified LB agar medium 1.5% micro agar (w/v) with or without antibiotics as selection markers at 37°C. The transformed *Agrobacterium* cells carrying gene of interest were cultured in the liquid LB medium (MERCK) or on solidified LB agar medium with appropriate antibiotics as selection markers at 28°C.

3. Enzymes and Chemicals

Restriction enzymes were purchased from New England Biolab (N.E.B) and used as recommended by the manufacturer. All reagents for polymerase chain reaction (PCR) and reverse transcription polymerase chain reaction (RT-PCR) were purchased from Thermo Fisher Scientific Inc. and Enzynomics company. Medium components for bacteria culture and plant culture and X-GlcA were purchased from DUCHEFA. Macerozyme R-10 and Cellulase R-10 were purchased from Yakult PHARMACEUTICAL INDUSTRY Co. Ltd. Other reagents were purchased from Sigma-Aldrich Company.

4. Isolation of nucleic acid

4.1 Plasmid DNA isolation from *E. coli*

A small quantity of plasmid DNA was isolated from 5 ml cultured *E. coli* cells by plasmid purification kit (NucleoSpin Mini Prep). For the isolation of a large amount of plasmid DNA, 200 ml of cultured *E. coli* cells were used to isolate DNA by plasmid purification kit (QIAGEN Plasmid Purification Maxi Kit).

4.2 Genomic DNA isolation

A small amount of genomic DNA used for PCR was isolated from 100 mg of *Arabidopsis thaliana* plant material using DNeasy Plant Mini Kit (QIAGEN) following the manufacturer's instructions.

4.3 Total RNA isolation for RT-PCR

Total RNA was isolated from 100 mg of *Arabidopsis* plant material using the RNeasy Plant Mini Kit (QIAGEN) according to the manufacturer's instructions. Genomic DNA was removed by DNase I (QIAGEN).

5. Bacterial transformation

5.1 *E. coli* Transformation

E. coli HIT^{TM} *DH5α* competent cells were purchased from Real Biotech Company. And the transformation was done according to the protocol provided.

5.2 *Agrobacterium tumefaciens* transformation

200 μl of *Agrobacterium GV3101* strain stock was inoculated into 40 ml of LB media contianing gentamycin (25 μg/ml) overnight at 28°C 2 ml of the cultured cells were removed into fresh LB media with gentamycin (25 μg/ml) and incubated for 4-6 hours. Then it was transferred into an autoclaved sorvall tube and centrifuged at 8,000 rpm at 4°C for 5 min. Supernatant was discarded and the pellet was suspended by 10 ml of 0.15 M NaCl and centrifuged for washing. Supernatant was discarded and the pellet was resuspended by 1 ml of 20 mM chilled $CaCl_2$. 100 μl of suspension was added to micro centrifuge tube with 1 μg DNA of interest. The mixture was tapped smoothly and incubated on ice for 30 min, followed by

incubation in the liquid nitrogen for 1min, and then in 37°C water bath for 5 min. 1 ml LB media was added into the tube and incubated in 28°C shaker for 4 hours, followed by centrifuging at 8,000 rmp for 1 min. 900 μl supernatant was removed and the remained pellet was resuspended, followed by plated on LB agar media with appropriate antibiotics and incubated for 2-3 days.

5.3 *Arabidopsis* transformation (The floral dipping)

Arabidopsis wild type plants were grown healthily until they were flowering. First blots could be chipped to encourage proliferation of many secondary blots in 4-6 days before transformation. *Agrobacterium tumefaciens* carrying gene of interest on a binary vector was grown in 5 ml of liquid media with gentamycin (25 μg/ml) and other appropriate antibiotics at 28°C for one day, then transferred into 300 ml of LB liquid media with gentamycin (25 μg/ml) and other appropriate antibiotics incubated at 28°C overnight. The liquid was transferred into 250 ml bottles and centrifuged at 8,000 rpm at 4°C for 10 min. The supernatant was discarded and the pellet was resuspended with 150 ml 5% sucrose solution (w/v). Silwet L-77 was add into the *Agrobacterium* solution with the concentration of 0.03% and mixed well. The above soil parts of *Arabidopsis* wild type plants were dipped in *Agrobacterium* solution for 5 seconds. The dipped plants were placed under a black dome for 16-24 hours to maintain high humidity. Dry seeds can be plated on MS media supplemented appropriate antibiotics as selection makers. The putative plants were transferred on soil to grow (Clough *et al*., 1998).

6. Genotyping PCR

The insertion site of the T-DNA in the activation tagging mutant *ATL98246* plant was confirmed by genotyping PCR with specific primer sets LB3, geno_LP and geno_RP and the insertion site of the T-DNA in the *CS878754* mutant plant was confirmed by specific primer sets LB3, salk line_LP and salk line_RP made by Cosmo Company. Specific primer sets used were listed in the primer table.

7. RT-PCR analysis

Specific primer sets used for RT-PCR analysis were designed by the primer3 web tool and ordered from Cosmo Company. Specific primer sets used were listed in the primer table.

Total RNA was prepared using the RNeasy Plant Mini Kit (QIAGEN) and quantified using the GeneQuant™ *pro* RNA/DNA Calculator Spectrophotometer (Amersham Biosciences). 2 μg of total RNA were used to synthesize cDNA using RevertAid First Strand cDNA Synthesis Kit (Frementas) following the manufacturer's instructions. The synthesized cDNA were subjected to PCR with *tubulin* gene used for normalization.

8. Recapitulation

Full length cDNA of the *At5g19700* gene was amplified by RT-PCR using the gene specific primers. The primer set DTX52 XbaI_5 and TX52 BamHI_3 used for the recapitulation of *At5g19700* gene were designed by the primer3 web tool and ordered from Cosmo Company. Specific primer set used was listed in the primer

table.

The *At5g19700* gene was subcloned into pJET vector by using CloneJET™ PCR Cloning Kit and transferred into *E. coli*, then digested with specific enzymes *Xba*I and *Bam*HI to cut the target gene from pJET cloning and cloned into pBI111-L binary vector, which was transferred into *Agrobacterium* and then transferred into wild type plants by the floral dipping method. The T1 transgenic seeds were selected on 50 mg/ml kanamycin (w/v) MS agar plates.

9. Histochemical GUS staining assay

The histochemical staining of GUS was carried out as reported by (Sessions *et al*., 1999; Basu *et al*., 2003). In order to construct the transcriptional line *pAt5g19700::GUS*, 2.4 kb promoter of the *At5g19700* gene was amplified by specific primer sets 2.4pAt5g19700_SalI_5 and 2.4pAt5g19700_BamhI_3, and subcloned into pJET vector using CloneJET™ PCR Cloning Kit and transferred into *E. coli*, then cloned into pBI101 binary vector, which was transferred into *Agrobacterium* and finally transferred into *Arabidopsis* wild type plants. T1 transgenic plants were selected on 50 mg/ml kanamycin (w/v) MS agar plates and the transcriptional pattern of the *At5g19700* gene was analyzed by GUS staining. Briefly, the histochemical GUS staining assay was performed in a staining solution [50 mM sodium phosphate buffer (pH 7.2), 2 M potassium ferrocyanide and ferricyanide, 0.1% Triton X-100 (v/v), 10 mM EDTA, 5 mg/ml X-GlcA (w/v) (5-bromo-4-chloro-3-indolyl-β-D-glucuronic acid)]. The samples were infiltrated under vacuum for 1 hour and then incubated at 37°C overnight. After staining

solution was removed, the samples were cleaned by ethanol series solution.

10. Microscopy

The tissues were prepared on slides with cover slips and observed with a Zesis Axio Imager A1 Microscope. Confocal images were taken with a Confocal Laser Scanning Microscope (LSM700). The XF116 filter set (exciter, 474AF20; dichroic, 500DRLP; emitter, 510AF23) was used.

11. Observation of subcellular localization

To examine the subcellular localization of the At5g19700 protein, the full-length *At5g19700* cDNA was fused with green fluorescent protein (GFP) in the *326GFP* vector to generate the *CaMV35S::At5g19700:GFP* construct. The *At5g19700* gene cDNA without the termination codon was prepared by PCR amplification using the wild type plants DNA as a template. The specific primers for the PCR amplification were At5g19700_XbaI and At5g19700_BamHI. The subceluular localization detection was established with the *CaMV35S::ATPase-H^+: RFP* construct of the plasma membrane marker ATPase-H^+ protein (Arango *et al.*, 2003). The fusion constructs were introduced into *Arabidopsis* protoplasts prepared from whole seedlings by polyethylene glycol–mediated transformation (Kang *et al.*, 1998).

Briefly, 3 to 4 week old wild type plants grown on MS medium containing 2% sucrose were cut with a new surgical blade and incubated in 25 mL of enzyme solution [0.25% Macerozyme (Yakult Honsha Co., Ltd., Tokyo, Japan) R-10, 1.0%

Cellulase (Yakult Honsha Co., Ltd.) R-10, 500 mM mannitol, 1 mM $CaCl_2$, 25 mg BSA and 5 mM Mes-KOH, pH 5.6] at 23°C for overnight with gentle shaking. After incubation, the protoplast suspension was filtered through 100-μm mesh and overlaid on top of 20 mL of 21% sucrose solution, and centrifuged at 730 rpm for 10 min at 4°C. The intact protoplasts at the top and middle interfaces were transferred to a new conical tube containing 20 mL of W5 solution [154 mM NaCl, 125 mM $CaCl_2$, 5 mM KCl, 5 mM glucose, and 1.5 mM Mes-KOH, pH5.6]. The protoplasts were collected by centrifugation at 530 rpm for 6 min at 4°C. After the centrifugation, remove the supernatant totally and the pelleted protoplasts were resuspended in 20 mL of W5 solution. The protoplasts were incubated for 3 to 4 hours at 4°C or on ice to pellet the protoplasts naturally.

To transfer the DNA of *CaMV35S::At5g19700:GFP* and *CaMV35S:: ATPase-H^+:RFP* constructs into protoplasts, protoplasts were resuspended in MaMg solution [400 mM mannitol, 15 mM $MgCl_2$, and 5 mM Mes-KOH, pH 5.6] after the supernatant was removed totally. Plasmid DNA (10 to 20 μg total at a concentration around 2 mg/mL) was added to 300 μL of protoplast suspension followed by 330 mL of PEG solution [400 mM mannitol, 100 mM $Ca(NO3)_2$, and 40% polyethylene glycol 8000]. The mixture was mixed gently and incubated for 30 min at room temperature. After incubation, the mixture was washed with 1 mL of W5 solution for 4 times every 10 min. The protoplasts were recovered by centrifugation at 500 rpm for 4 min, resuspended in 2 mL of W5 solution, and incubated at 24°C (Lee *et al.*, 2008; Lee *et al.*, 2003).

Table1. List of primer sequences used in this study.

Oligo name	Sequence
LB3	5’-TTGACCATCATACTCATTGCTG-3’
geno_LP	5’-TGCCAGCTTTGAGAAATGTG-3’
geno_RP	5’-ATGGTGATCAAATCCCTCCA-3’
salk line_LP	5’-TAAAATATCACGTGGCGTTCG-3’
salk line_RP	5’-GAGGGTGAAGAAAGGAATTGG-3’
At5g19700RT_LP	5’-TACCCAAAGTCCGCAAAATC-3’
At5g19700RT_RP	5’-ATGGAAACCCCAAACATCATC-3’
At5g19710_LP	5’-ATGGTGATCAAATCCCTCCA-3’
At5g19710_ RP	5’-GCTACATCTGTTGGACCAGCTT-3’
At5g19720_LP	5’-TGATGCTAAAAGATGGCCTGAT-3’
At5g19720_RP	5’-CTATTTCCCACCTTTCTTGTAGCC-3’
TUB_FOR	5’-CTCAAGAGGTTCTCAGCAGTA-3’
TUB_REV	5’-TCACCTTCTTCATCCGCAGTT-3’
DTX52 XbaI_5	5’-GACTCTAGAGGAATGGAAACCCCAAACATC-3’
DTX52 BamHI_3	5’-GCCGGATCCCGGGTCAGTAGCGACAGTGAC-3’
2.4pAt5g19700_SalI_5	5’-GTCGACGATGTAGCTGTGAATTCAAGCTG-3’
2.4pAt5g19700_BamhI_3	5’-GCCGGATCCCGGGTCAGTAGCGACAGTGAC-3’
DTX52_Bamh1_3	5’-GCCGGATCCCGGGTCAGTAGCGACAGTGAC-3’
At5g19700_XbaI	5’-TCTAGAATGGAAACCCCAAACATC-3’
At5g19700_BamHI	5’-GGATC GTCAGTAGCGACAGTGAC-3’
IAA1_F	5’-TGGACGGAGCTCCATATCTC-3’
IAA1_R	5’-ATCACCGACCAACATCCAAT-3’
IAA2_F	5’-CGGATCCCTTCATGATTCTG-3’
IAA2_R	5’-TGTCTTGGATTACCCGGAAG-3’
IAA5_F	5’-GCACGATCCAAGGAACATTT-3’
IAA5_R	5’-TCACCGAACTACGGCTAGGT-3’
IAA6_F	5’-TTCACGATCCTCAGCCTCTT-3’
IAA6_R	5’-GAGGGTGCTCTCGGATATGA-3’
IAA19_F	5’-GGCTTGAGATAACGGAGCTG-3’
IAA19_R	5’-AACCTTCTCAGCGTCACCAC-3’

RESULTS

1. The phenotypes with the ATL98246 mutant plant was phenocopied in the recapitulation plant

To confirm whether overexpression of the *At5g19700* gene is responsible for the *ATL98246* mutant plant phenotypes, full length cDNA of the *At5g19700* gene was amplified and then cloned into downstream of the *CaMV 35S* enhancers of the binary pBI111-L vector to generate the *35S::At5g19700* construct to recapitulate the phenotypes of the *ATL98246* mutant plant. T1 transgenic lines were selected by kanamycin antibiotics on MS medium and at least twenty F2 independent transgenic lines were obtained. The F2 generation of recapitulated plants phenocopied the fast-growth, bushy dwarf and reduced apical dominance with multiple branching phenotypes which resemble the *ATL98246* mutant plant. The number of rosette-leaf branches and cauline-leaf branches were increased, the plant height and seed number were reduced (Figure 3A and B). In addition, the transcription level of the *At5g19700* gene in the 4 week old whole plants was detected through RT-PCR analysis. The results indicated that the transcription level of the *At5g19700* gene was increased in the transgenic lines than that in wild type plant (Figure 3C).

Therefore, these results support that up-regulated expression of the *At5g19700* gene activated by the *CaMV 35S* enhancers on the T-DNA is responsible for the phenotypes of the *ATL98246* mutant plant.

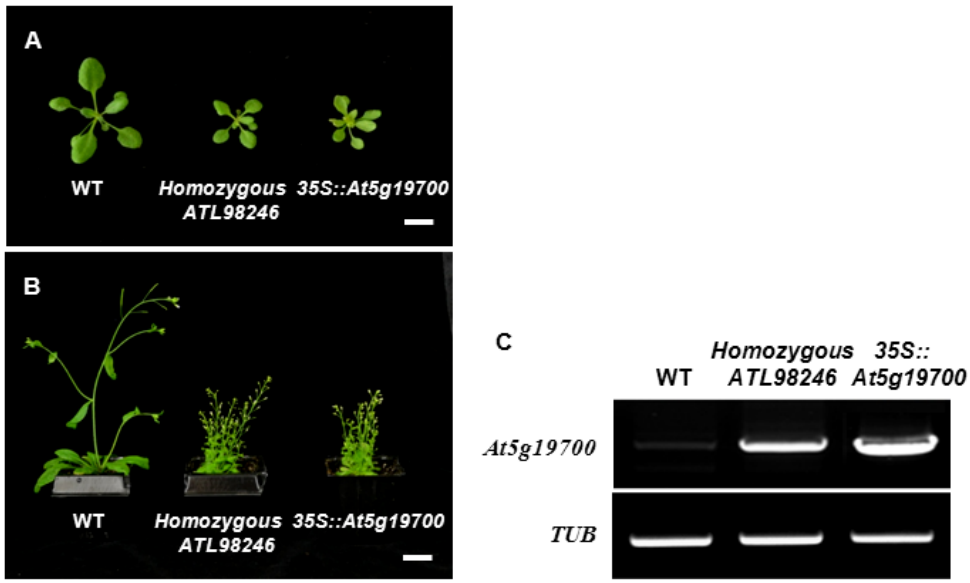

Figure 3. The multiple branching phenotype was rescued in the recapitulated plant

(A) Phenotypes of 2 week old *35S::At5g19700* recapitulation plant compared with wild type and homozygous *ATL98246* mutant plants. Scale bar: 1 cm.

(B) Severe reduced apical dominance phenotypes of 4 week old *35S::At5g19700* recapitulated plants compared with wild type and homozygous *ATL98246* mutant plants. Scale bar: 1 cm.

(C) The transcription levels of the *At5g19700* gene in wild type, homozygous *ATL98246* mutant and *35S::At5g19700* recapitulated plants. RNA isolated from 4 week old whole plants was used for the RT-PCR analysis.

The *Tubulin* gene was used for normalization.

2. The At5g19700 protein is a member of the MATE protein family

The At5g19700 protein is a member of the MATE transporter protein family. Multidrug and toxic compound extrusion (MATE) is a family of transporter proteins, which is widely distributed in all living kingdoms. Although the length of proteins in the MATE family ranges from 400 to 700 amino acids, most members consist of 400-500 residues with 10 to 12 transmembrane helices. The plant MATE family has large members of orthologues, with the existence of 56 members in the *Arabidopsis*. At5g19700 was referred to AtDTX52 (for *Arabidopsis thaliana* Detoxification 52). With the whole-genome sequences being completed, the most closely homologous of At5g19700/AtDTX52 protein in other plants is Os3g0227966 protein in *Oryza sativa Japonica Group*, which has 50% identity and 69% similarity of amino acid sequences with At5g19700/AtDTX52 protein. And the most similar *Arabidopsis* protein to At5g19700/AtDTX52 is At4g29140/AtDTX51 protein with 67% identity and 80% similarity of the amino acid sequences, analyzed by the NCBI BLAST tool.

Arabidopsis thaliana processes 56 MATE transporter members. The rooted phylogenetic tree with branch length analyzed by the UPGMA method shows the amino acid sequence similarity of the At5g19700 protein with other 55 members of the MATE family (Figure 4A). Amino acid sequences of these 56 MATE family members were aligned using the ClustalW (http://www.genome.jp/tools/clustalw/) tools. All MATE proteins share protein sequence similarity up to 40%. However, no apparent consensus sequence is conserved in the MATE family members. The

phylogenetic tree of 56 MATE members shows 9 proteins including At5g19700 protein in one genetic cluster of evolution. Therefore, other eight MATE proteins closer to At5g19700 protein were analyzed. Figure 4B indicates the phylogenetic tree of these eight MATE family members, At1g58340 (AtDTX48/AtBCD1/AtZRZ), At4g23030 (AtDTX49), At5g52050 (AtDTX50), At4g29140 (AtDTX51/AtADS1), At2g38510 (AtDTX53) At1g71870 (AtDTX54), At5g49130 (AtDTX55), At4g22790 (AtDTX56) and their relationship with At5g19700 (AtDTX52) protein. The alignment of the amino acid sequences were analyzed by the ClustalW (http://www.genome.jp/tools/clustalw/) tool. The sequence analysis of the encoded protein showed that the At5g19700 protein is highly homologous with these eight MATE proteins in the MATE super family (Figure 5).

The *At5g19700* gene is 1527 bp in length without intron and encodes a predicted protein of 508 amino acids. In *silico* analysis using HMMTOP transmembrane topology prediction, the *At5g19700* gene encodes a membrane protein with 12 potential α-helical transmembrane domains (Figure 6). Figure 6A shows the amino acid sequences of the 12 α-helical transmembrane motifs with prediction underlined and marked as I—XII. Figure 6B shows the topology prediction of the At5g19700 protein structure by HMMTOP in that 12 potential α-helical transmembrane domains are marked as I—XII and both of the N terminal and C terminal are out of the cytoplasm.

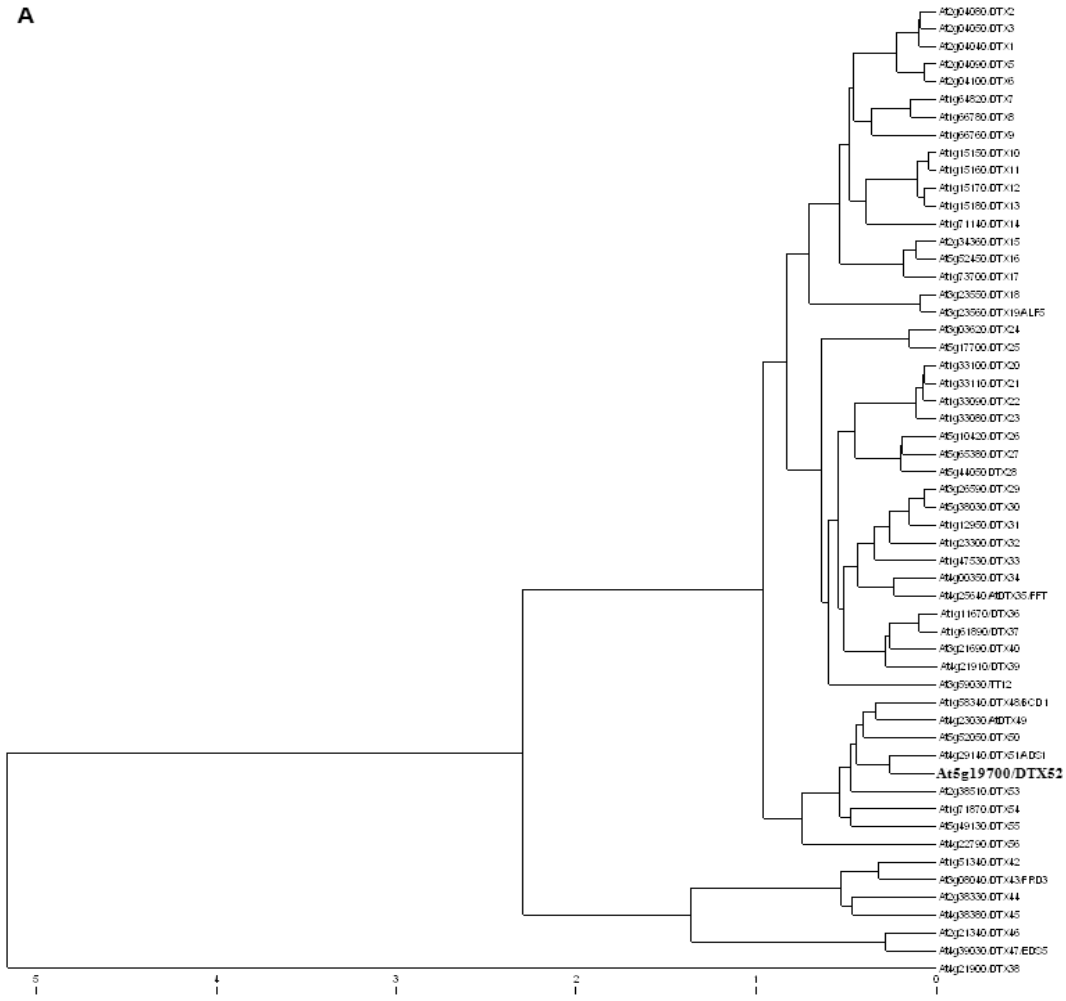
A
At2g04080.0TX2
At2g04050.0TX3
At2g04040.0TX1
At2g04090.0TX5
At2g04100.0TX6
At1g64820.0TX7
At1g66780.0TX8
At1g66760.0TX9
At1g15150.0TX10
At1g15160.0TX11
At1g15170.0TX12
At1g15180.0TX13
At1g71140.0TX14
At2g34360.0TX15
At5g52450.0TX16
At1g73700.0TX17
At5g23550.0TX18
At5g23560.0TX19ALF5
At5g03620.0TX24
At5g17700.0TX25
At1g33100.0TX20
At1g33110.0TX21
At1g33090.0TX22
At1g33080.0TX23
At5g10420.0TX26
At5g65380.0TX27
At5g44050.0TX28
At5g26590.0TX29
At5g38030.0TX30
At1g12950.0TX31
At1g23300.0TX32
At1g47530.0TX33
At4g00350.0TX34
At4g25640.4fDTX35.FFT
At1g11670.0TX36
At1g51890.0TX37
At5g21690.0TX40
At4g21910.0TX39
At5g59030.TT12
At1g58340.0TX48.6CD1
At4g23030.4fDTX49
At5g52050.0TX50
At4g29140.0TX51.ADS1
At5g19700/DTX52
At2g38510.0TX53
At1g71870.0TX54
At5g49130.0TX55
At4g22790.0TX56
At1g51340.0TX42
At5g08040.0TX43.FRD3
At2g38330.0TX44
At4g38380.0TX45
At2g21340.0TX46
At4g39030.0TX47.EDS5
At4g21900.0TX38
5
4
3
2
1
0

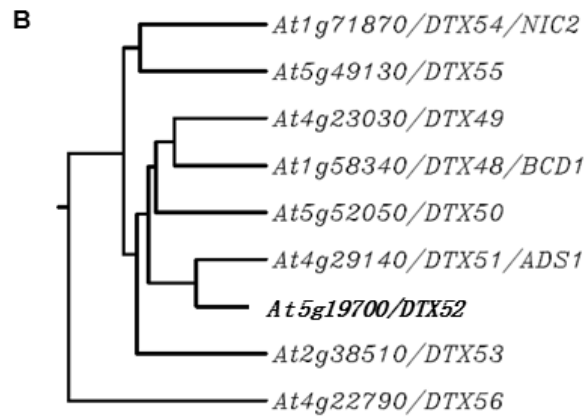

Figure 4. The phylogenetic tree of 56 members in the MATE superfamily

(A) Amino acid sequences of 56 MATE family members were aligned using the ClustalW (http://www.genome.jp/tools/clustalw/) tools. The rooted phylogenetic tree with branch length (UPGMA) shows the amino acid sequence similarity relationship of the At5g19700 protein with other 55 members of MATE family proteins.

(B) The rooted phylogenetic tree with branch length (UPGMA) of nine proteins in one genetic cluster of evolution including the At5g19700 protein as indicated by number.

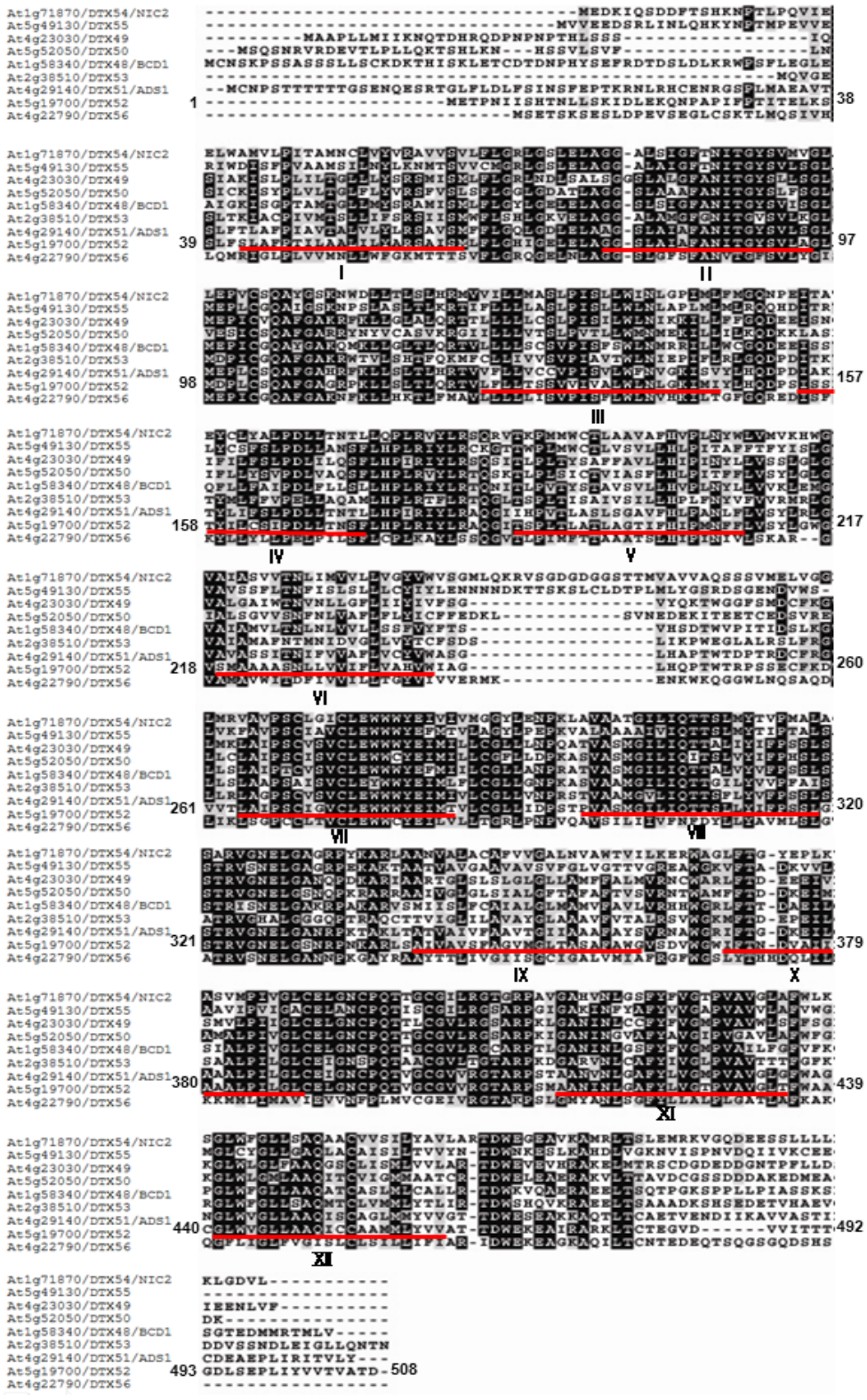
At1g71870/DTX54/NIC2
At5g49130/DTX55
At4g23030/DTX49
At5g52050/DTX50
At1g58340/DTX48/BCD1
At2g38510/DTX53
At4g29140/DTX51/ADS1
At5g19700/DTX52
At4g22790/DTX56
I
II
III
IV
V
VI
VII
VIII
IX
X
XI
XII

Figure 5. The multiple sequence alignment of the At5g19700 protein with other eight MATE proteins

Amino acid sequences were aligned using the ClustalW (http://www.genome.jp/tools/clustalw/) and BoxShade (http://www.ch.embnet.org/software/BOX_form.html) tools. Amino acids are indicated by the standard single latter designation, and dashes indicate gaps. Residues that are absolutely conserved are shaded in black, and biochemically conserved residues are shaded in grey. The transmembrane motifs of the At5g19700 protein are underlined and marked I–XII. Numbers are residue positions of the At5g19700 protein.

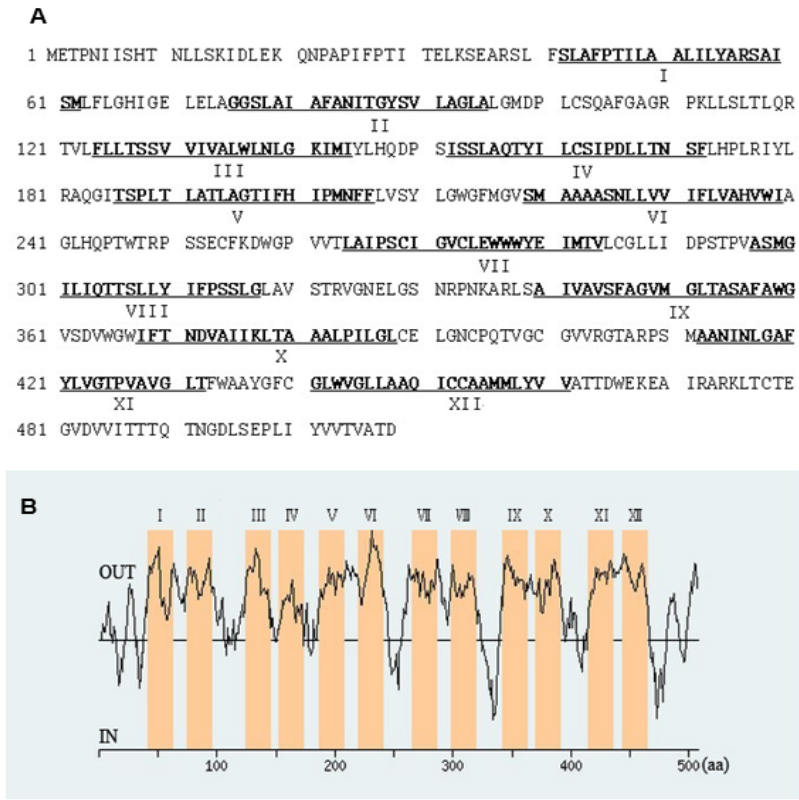

Figure 6. The potential transmembrane motifs and hydrophobic plot prediction of the At5g19700 MATE protein

(A) Amino acid sequence of At5g19700 protein. Residues constituting the transmembrane motifs are underlined and marked as I–XII. Numbers are residue positions.

(B) The hydrophobic plot of the At5g19700 protein was predicted using HMMTOP transmembrane topology prediction. The 12 transmembrane motifs are marked I–XII. aa: amino acids.

3. The At5g19700 gene is expressed in the whole plant and strongly expressed in siliques

As mentioned above, At5g19700 protein belongs to the MATE transporter family in which the expression of the member genes are quite diverse. In order to investigate the expression pattern of the *At5g19700* gene, total RNA was isolated from rosette leaves, cauline leaves, stems, flowers, siliques and roots of wild type plants. The transcription levels of the *At5g19700* gene in different tissues were detected by RT-PCR analysis. As shown in Figure 7A, the *At5g19700* gene was expressed in the rosette leaves, cauline leaves, roots, flowers and stems, and was highly expressed in siliques.

To examine more specific expression patterns of the *At5g19700* gene, the transcriptional fusion of *At5g19700* to the β-glucuronidase (*GUS*) reporter gene was introduced into *Arabidopsis* plants. Plant researchers have detected tissues using *GUS* reporter gene fusions for transient expression studies in order to better understand promoter-specified developmental gene expression pattern. In this study, the transcriptional fusion *pAt5g19700::GUS* construct contains the 2.4 kb promoter sequence upstream of the *At5g19700* gene. The activitis of GUS reporter were detected in seedlings, flowers and siliques of the ten individual lines of T2 generation *pAt5g19700:: GUS* transgenic plants grown in the long day condition by the histochemical GUS staining assay. GUS activity was showed in leaves, roots, floral clusters and siliques among the ten individual lines (Figure 7B to I). In the leaf, GUS activity was shown in primordia and venation (Figure 7B and C). In the

root, GUS activity was shown in the central vascular cylinder (Figure 7D and E). In the floral cluster, GUS signal was detected in the early stage anther, the style and the filament of stamen (Figure 7F, G and H).

In addition, the specialized expression pattern in the developing seeds was analyzed in more detail. In the developing seeds, GUS activity was observed in the chalazal endosperm. GUS staining was performed in different stages in the developing seeds around from 1 day after fertilization (DAF). The developmental age of immature seeds prior to the globular stage were judged by seed size, silique length and silique location relative to the inflorescence. GUS activity was shown in the chalazal endosperm of the seed 1 day after fertilization (DAF), the globular stage and the heart stage of developing seeds (Figure 7J, K and L). The chalazal endosperm cyst (CEC) is mushroom-shaped with a globular head and a branched basal portion like a short tentacle that is separated from the cellularized endosperm. From the 4 DAF stage, cellularization starts in the chalazal endosperm and GUS signal was deleted (Figure 7M and N).

Taken together, these results imply that the *At5g19700* gene was expressed in the rosette leaves, cauline leaves, stems, roots, floral clusters and siliques of the plant and strongly expressed in the chalazal endosperm of developing seeds in *Arabidopsis*.

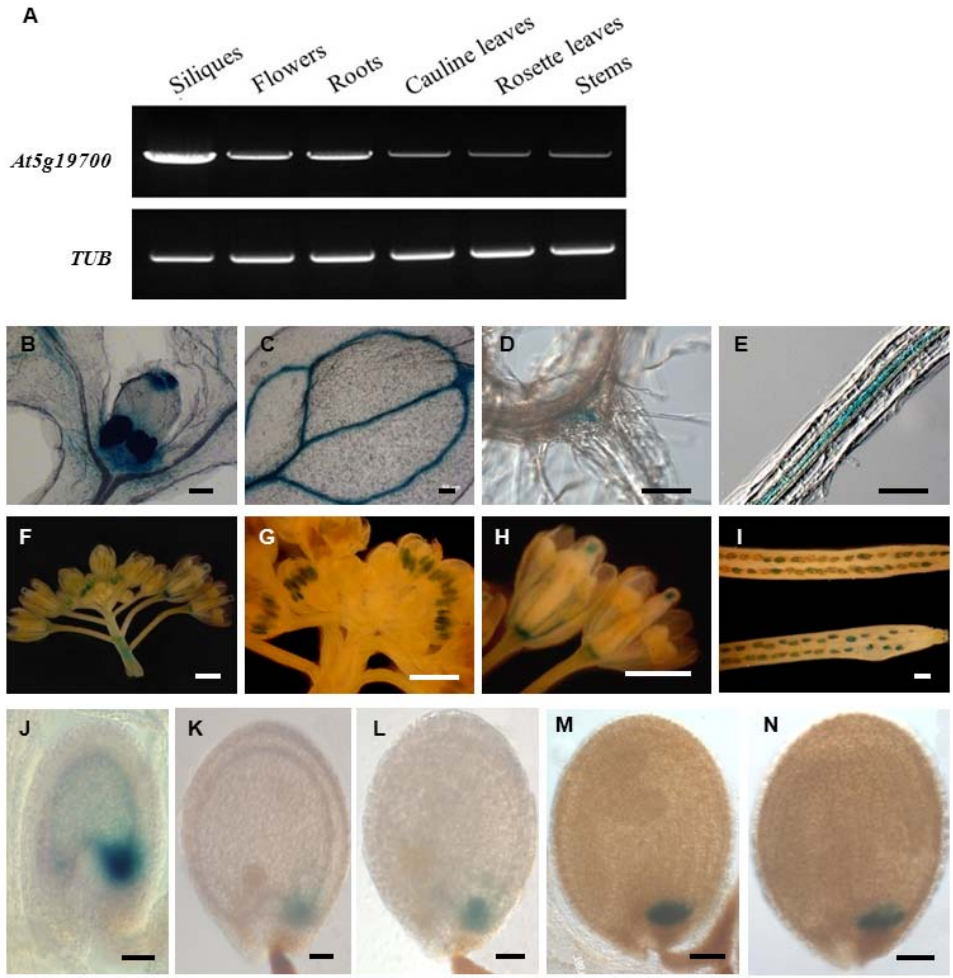

Figure 7. The expression pattern of the *At5g19700* gene in *Arabidopsis*

(A) RT-PCR analysis of special expression patterns of the *At5g19700* gene in various organs: siliques, flowers, roots, cauline leaves, rosette leaves and stems. The *tubulin* gene was used for normalization.

(B) GUS staining in a 7 day old seedling of the transcriptional line. GUS activity was shown in primordia of young leaves. Scales bar: 50 μm.

(C) GUS staining in a 7 day old seedling of the transcriptional line. GUS activity was shown in leaf venation. Scales bar: 50 μm.

(D) GUS staining in a 7 day old seedling of the transcriptional line. GUS activity was shown in root. Scales bar: 50 μm.

(E) GUS staining in a 7 day old seedling of the transcriptional line. GUS activity was shown in the central vascular cylinder of root. Scales bar: 50 μm.

(F) GUS staining in a 6 week old plant of the transcriptional line. GUS activity was shown in floral clusters. Scales bar: 2 mm.

(G) GUS staining in a 6 week old plant of the transcriptional line. GUS activity was shown in early stage flowers. Scales bar: 2 mm.

(H) GUS staining in a 6 week old plant of the transcriptional line. GUS activity was shown in the style and the filament of stamen in flowers. Scales bar: 2 mm.

(I) GUS staining in a 6 week old plant of the transcriptional line. GUS activity was shown in siliques. Scales bar: 2 mm.

(J) GUS staining in 1 DAF developing seeds of the transcriptional line. GUS activity was shown activity in chalazal endosperm. Scales bar: 50 μm.

(K) GUS staining in 2 DAF developing seeds of the transcriptional line. GUS activity was shown in chalazal endosperm. Scales bar: 50 μm.

(L) GUS staining in 3 DAF developing seeds of the transcriptional line. GUS activity was shown in chalazal endosperm. Scales bar: 50 μm.

(M) GUS staining in 4 DAF developing seeds of the transcriptional line. GUS activity was shown in chalazal endosperm. Scales bar: 100 μm.

(N) GUS staining in after 5 DAF developing seeds of the transcriptional line. GUS activity was shown in chalazal endosperm. Scales bar: 100 μm.

4. The subcellular localization of At5g19700 protein is on the membrane of vacuole

The subcellular localization of some members of MATE family had been studied to have transport functions in *Arabidopsis*. Analysis of the signal peptide of the At5g19700 amino acid sequence using the subcellular prediction programs SIG Pred (http://bmbpcu36.leeds.ac.uk/prot_analysis/Signal.html) and MultiLoc/ TargetLoc (http://www-bs.informatik.uni-tuebingen.de/Services/MultiLoc/) revealed that the possible cleavage position is between the 58^{th} and 59^{th} amino acid, and the most chance of the protein targeting is in the vacuolar; however, the prediction score got just 0.28.

To examine the subcellular localization of At5g19700 protein, the *CaMV35S::At5g19700:GFP* plasmids and the plasma membrane marker *CaMV35S::ATPase-*H^+*:RFP* plasmids were introduced into *Arabidopsis* protoplasts prepared from leaf mesophyll by polyethylene-glycol mediated transformation. After incubation for 24 h at 22°C, images were taken using a cooled CCD camera coupled to a Zeiss Axioplan2 fluorescence microscope. The GFP signal of *CaMV35S::At5g19700:GFP* fusion was located in the vacuolar memberane (Figure 8A), while the RFP signal of *CaMV35S::ATPase-*H^+*:RFP* fusion was located on the plasma membrane (Figure 8B). Figure 8C is the merged picture of brightness. The fluorescence microscopy analysis revealed that the At5g19700 protein is located on the membrane of vacuole (Figure 8).

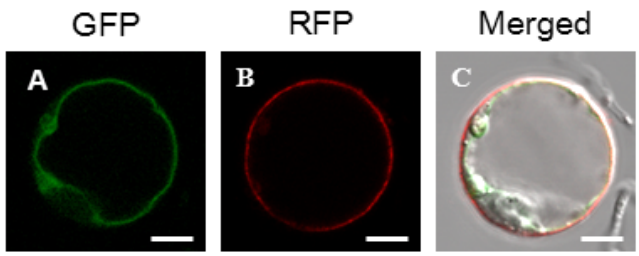

Figure 8. The subcellular localization of the At5g19700 protein

At5g19700::GFP and *ATPase-H$^+$::RFP* fusions were expressed in *Arabidopsis* protoplasts and observed by Confocal Laser Scanning Microscope (LSM700).

(A) Fluorescent image of protoplast under green chlorophyll fluorescence.

(B) Fluorescent image of protoplast under red chlorophyll fluorescence.

(C) Merge image of green and red chlorophyll fluorescence in bright field.

Scale bar: 20 μm.

5. Characterization of the knockout *CS878754* mutant plant

The T-DNA insertional *CS878754* (SAIL_1236_H10) mutant seed was gained from the ABRC (*Arabidopsis* Biological Resource Center, Ohio State University, Columbus, OH, U.S.A.). In the *CS878754* mutant plant, pDAP101 vector was inserted into the *At5g19700* gene (Figure 9A) to create the SAIL line. Genotyping PCR analysis was taken to confirm the T-DNA insertion in separate homozygous and heterozygous *CS878754* mutant plants (Figure 9B). RT-PCR analysis revealed that the *At5g19700* gene was not expressed in the *CS878754* mutant plant (Figure 9C). However, between wild type and *CS878754* plants there were not any visible phenotype difference appearing in 2 week old, 4 week old and 7 week old growth stages, which may indicate genetic redundancy in the MATE large family (Figure 9D, E and F). Genetic redundancy, which is due to the existence of several genes in the genome of an organism that perform the same role to some extent, should be the explanation for this situation. In this case, mutations or defects in one of these genes will have a smaller effect on the organism than expected from the genes' function. In the *CS878754* mutant, there can be little effect on phenotypes as a result of genetic redundancy.

The *CS878754* mutant plant being not affected in any other developmental architecture indicates that the *At5g19700* gene function could be redundant with other MATE family members of in *Arabidopsis.*

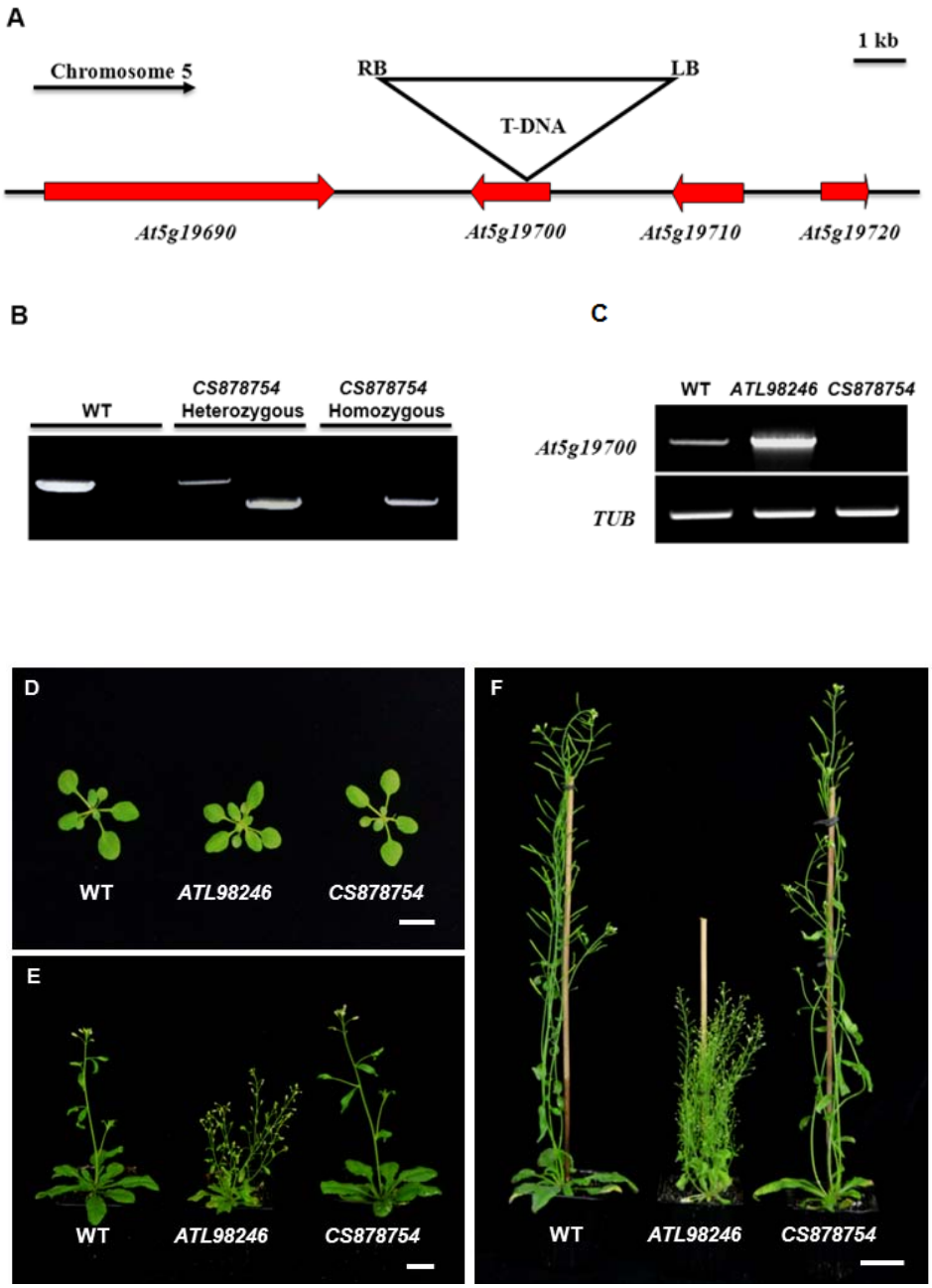
A
Chromosome 5
RB
LB
1 kb
T-DNA
At5g19690
At5g19700
At5g19710
At5g19720
B
WT
CS878754
Heterozygous
CS878754
Homozygous
C
WT
ATL98246
CS878754
At5g19700
TUB
D
WT
ATL98246
CS878754
E
WT
ATL98246
CS878754
F
WT
ATL98246
CS878754

Figure 9. The T-DNA insertion site, expression level of *At5g19700* gene and phenotypic comparison between wild type and the T-DNA insertional *CS878754* mutant plants

(A) The T-DNA insertion site in the T-DNA insertional *CS878754* mutant plant obtained from ABRC. T-DNA was inserted into the *At5g19700* gene. Scale bar: 1 kb DNA length.

(B) Genotyping PCR analysis of wild type, heterozygous and homozygous *CS878754* mutant plants.

(C) RT-PCR analysis of *At5g19700* gene expression levels in wild type, homozygous *ATL98246* and homozygous *CS878754* mutant plants. The RNA isolated from 4 week old whole plants was used for RT-PCR analysis.
The *tubulin* gene was used for normalization.

(D) View of 2 week old plants grown under the long day condition. From left to right: wild type, *ATL98246* mutant and homozygous *CS878754* mutant plants. Scale bar: 1 cm.

(E) View of 4 week old plants grown under the long day condition. From left to right: wild type, *ATL98246* mutant and homozygous *CS878754* mutant plants. Scale bar: 1 cm.

(F) View of 7 week old plants grown under the long day condition. From left to right: wild type, *ATL98246* mutant and homozygous *CS878754* mutant plants.
Scale bar: 1 cm.

9. The alternation of the expression level of *IAA* genes in the *ATL98246* mutant plant

Auxin, as one of the main hormones that move throughout the plant to control the shoot branching, plays a key role in plant developmental processes. Depending on the *ATL98246* mutant plant showing the reduced apical dominance and related phenotypes, RT-PCR analysis was carried out to examine the auxin-inducible gene expression levels in different plant tissues. The response of most members of the auxin/indole-3-acetic acid (Aux/IAA) family to auxin is rapid and the Aux/IAA family members are proposed to mediate tissue-specific and cell-type restricted responses to the hormone during plant growth and development (Abel *et al.*, 1995).

Auxin-inducible genes *IAA1*, *IAA2*, *IAA5*, *IAA6* and *IAA19* of the Aux/IAA family were examined by RT-PCR analysis in the whole plants, siliques, flowers, meristems, axillary buds and roots in wild type, *ATL98246* mutant and *CS878754* mutant plants. The results demonstrated that the expression levels of these genes were not changed in the 4 week old whole plants of the *ATL98246* and *CS878754* plants (Figure 10A). However, in different tissues the expression patterns were altered specifically. In siliques, the expression levels of the *IAA1*, *IAA6* and *IAA19* genes were down-regulated in the *ATL98246* mutant, but the *IAA19* gene was decreased mostly in the *ATL98246* mutant (Figure 10B). The expression levels of *IAA5* gene in the flowers, axillary buds and shoot apexes was mostly down-regulated in the *ATL98246* mutant and elevated in the *CS878754* mutant slightly (Figure 10C, D and E). The *IAA6* gene was decreased in the *ATL98246*

mutant comparing with wild type plant in axillary buds, shoot apexes and roots (Figure 10 D, E and F).

Among wild type, *ATL98246* mutant and *CS878754* mutant plants, the expression levels of some IAA-inducible genes showed variations. It is possible that auxin might be involved in the multiple branching phenotypes in the *ATL98246* mutant plant.

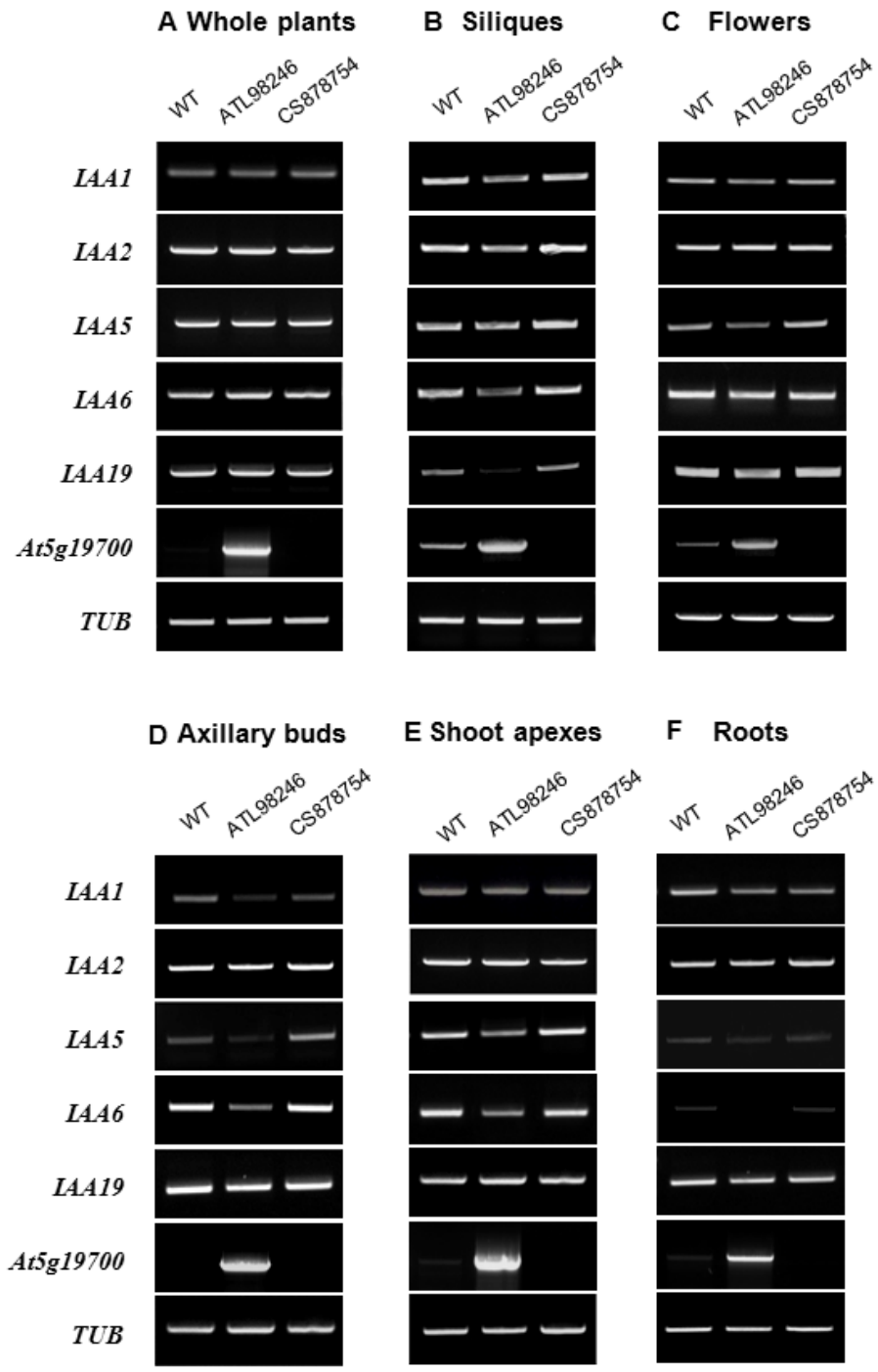
A Whole plants
B Siliques
C Flowers
WT
ATL98246
CS878754
IAA1
IAA2
IAA5
IAA6
IAA19
At5g19700
TUB
D Axillary buds
E Shoot apexes
F Roots

Figure 10. The RT-PCR analysis of auxin-inducible genes in wild type, *ATL98246* and *CS878754* mutant plants

(A) Expression levels of auxin-inducible genes *IAA1*, *IAA2*, *IAA5*, *IAA6* and *IAA19* in whole plants of wild type, *ATL98246* and *CS878754* mutant plants.

(B) Expression levels of auxin-inducible genes *IAA1*, *IAA2*, *IAA5*, *IAA6* and *IAA19* in siliques of wild type, *ATL98246* and *CS878754* mutant plants.

(C) Expression levels of auxin-inducible genes *IAA1*, *IAA2*, *IAA5*, *IAA6* and *IAA19* in flowers of wild type, *ATL98246* and *CS878754* mutant plants.

(C) Expression levels of auxin-inducible genes *IAA1*, *IAA2*, *IAA5*, *IAA6* and *IAA19* in axillary buds of wild type, *ATL98246* and *CS878754* mutant plants.

(D) Expression levels of auxin-inducible genes *IAA1*, *IAA2*, *IAA5*, *IAA6* and *IAA19* in shoot apexes of wild type, *ATL98246* and *CS878754* mutant plants.

(E) Expression levels of auxin-inducible genes *IAA1*, *IAA2*, *IAA5*, *IAA6* and *IAA19* in roots of wild type, *ATL98246* and *CS878754* mutant plants.

The *tubulin* gene was used for normalization.

DISSCUSSION

In this study, an *ATL98246* mutant plant with a multiple branching phenotype was isolated from activation tagging lines of *Arabidopsis* Columbia ecotype (Figure 1). The mutant plant exhibited fast-growth, bushy dwarf and reduced apical dominance phenotypes in the long day condition. The *ATL98246* mutant plant shows shorter siliques than those of wild type plant. Both the number of rosette-leaf branches and cauline-leaf branches of the *ATL98246* mutant plant are increased and the height of the plants is much reduced comparing with wild type plant.

The insertion site of T-DNA was identified by plasmid rescue, that the T-DNA was located in about 500 bp downstream of the start codon of *At5g19710* gene in the chromosome 5 (Figure 2). RT-PCR analysis confirmed that the expression level of the *At5g19700* gene was up-regulated by the *CaMV 35S* enhancer in the T-DNA. Recapitulated plants of the *At5g19700* gene expressed under the *CaMV 35S* promoter rescued the activation-tagged mutant phenotypes, which proved that the up-regulation of the *At5g19700* expression was responsible for the multiple branching phenotype of the *ATL98246* mutant plant (Figure 3). However, the knockout *CS878754* mutant plant does not show any different visible phenotype, even though the *At5g19700* gene was not expressed in the *CS878754* mutant plant, which indicated the extensive redundant activities of the *At5g19700* homologous genes (Figure 9).

The *At5g19700* gene encodes a member of the multidrug and toxic compound extrusion (MATE) transporter family (Figure 4). The plant MATE family has large members of orthologus, with the existence of 56 members in the *Arabidopsis*. The most closely homologous of At5g19700 protein in other plants is Os3g0227966 protein in *Oryza sativa Japonica Group*, and the most similar *Arabidopsis* protein is AtDTX51/At4g29140) protein (Figure 5). The *At5g19700* gene is 1527 bp in length without intorn and encodes a predicted protein of 508 amino acids membrane protein with 12 potential α-helical transmembrane domains predicted by HMMTOP transmembrane topology prediction (Figure 6).

The result of expression pattern detection by RT-PCR analysis indicates that the *At5g19700* gene is expressed in the roots, rosette leaves, cauline leaves and floral clusters with weaker transcription levels and expressed in the siliques strongly. The further histochemical GUS staining assay of *pAt5g19700::GUS* transgenic plants detected GUS signal in the primordia and venation of leaves, the central vascular cylinder of roots, the stigma and the filament of stamen in flowers, and the chalazal endosperm of developing seeds (Figure 7). The fluorescence microscopy observation of the subcellular localization of the *35S::At5g19700:GFP* fusion with the *35S::ATPase-H^+:RFP* fusion as a plasma membrane located marker revealed that the subcellular localization of At5g19700 protein was the membrane of the vacuole (Figure 8).

In the *ATL98246* mutant plant, the expression levels of auxin-inducible *Aux/IAA* genes have some alternations in the siliques, flowers, axillary buds, shoot

apexes and roots (Figure 10). The *Aux/IAA* genes regulate various auxin responses through auxin perception. The *Aux/IAA* genes are rapidly induced in response to auxin (Reed 2001; Brunoud *et al.,* 2012). Auxin induces different *Aux/IAA* genes to varying degrees and with different kinetics. The differences in sensitivity of transcript accumulation and kinetics between individual *IAA* genes are likely due to a variety of factors, such as issue-specific expression, cell-type dependent, tissue-specific auxin permeability, and differential regulation of free auxin concentrations, or different modes of auxin-dependent transcriptional activation and post-transcriptional regulation. In this study, the expression levels of *IAA5* gene in the flowers, axillary buds and shoot apexes were down-regulated in *ATL98246* mutant plant comparing with wild type plant. The *IAA6* gene expression was decreased in axillary buds, shoot apexes of the *ATL98246* mutant. The *IAA6* gene was specifically changed in the roots and the*IAA19* gene was specifically changed in the siliques of the *ATL98246* mutant. Some studies suggested that auxin induces the expression of many, but not all, *Aux/IAA* gene family members. *IAA* genes are not involved in the same biological pathways. For instance, although *IAA5*, *IAA6*, and *IAA19* genes share sequence similarity, their expression patterns show distinct tissue specificity. *IAA5* is mainly expressed in seedling and shoot; *IAA6* gene is expressed in seedling and flowers; and *IAA19* gene is specifically expressed in flowers. None of the three *IAA* genes exhibit significant correlative expression profiles with each other (Overvoorde *et al.,* 2005). In the *ATL98246* mutant plant, the specific alternation of *IAA* genes suggested that auxin might be

involved in the multiple branching phenotype in the *ATL98246* mutant plant.

However, as a MATE family member, any mechanism of transport function of At5g19700 protein has not been built yet. The subcelluar localization of some MATE proteins was found to be located on various cell membranes and only a few MATEs were described as a transporter. For example, the AtDTX1 is present in the plasma membrane mediating export of exogenous toxic compounds. The TT12 protein is thought to be localized on the vacuolar membrane, where it controls the sequestration of flavonoids, the anthocyanin transport The BCD1 protein is known as an iron transporter localized on Golgi complex contributing to iron homoeostasis during stress response and senescence. Even though At5g19700 protein was found to be located on the membrane of vacuole, the transport function of this MATE is still not known to be related to the multiple branching phenotype in this *ATL98246* mutant plant.

REFERENCES

Abel, S., Nguyen, M.D., and Theologis, A. (1995). The PS-IAA4/5-like family of early auxin-inducible mRNAs in *Arabidopsis thaliana*. J Mol Bio *251*, 533-549.

Agustia, J., Herold, S., Schwarz, M., Sanchez, P., Ljung, K., Dun, E.A., Brewer, P.B., Beveridge, C.A., Sieberer, T., Sehr, E.M., and Greb, T. (2011). Strigolactone signaling is required for auxin-dependent stimulation of secondary growth in plants. Proc Natl Acad Sci U S A *108*, 20242-20247.

Arango, M., Gévaudant, F., Oufattole, M., and Boutry, M. (2003). The plasma membrane proton pump ATPase: the significance of gene subfamilies. Planta *216*, 355-365.

Basu, C., Kausch, A.P., Luo, H., and Chandlee, J.M. (2003). Promoter analysis in transient assays using a GUS reporter gene construct in creeping bentgrass (Agrostis palustris). Plant Physiol *160*, 1233-1239.

Bennett, T., Sieberer, T., Willett, B., Booker, J., Luschnig, C., and Leyser, O. (2006). The *Arabidopsis* MAX pathway controls shoot branching by regulating auxin transport. Curr Biol *16*, 553-563.

Brown, D.E., Rashotte, A.M., Murphy, A.S., Normanly, J., Tague, B.W., Peer, W.A., W.A., Taiz, L., and Muday, G.K. (2001). Flavonoids Act as Negative Regulators of Auxin Transport in Vivo in Arabidopsis. Plant Physiol *126*, 524-535

Brunoud, G., Wells, D.M., Oliva, M., Larrieu, A., Mirabet, V., Burrow, A.H.,

Beeckman, T., Kepinski, S., Traas, J., Bennett, M.J., and Vernoux, T. (2012). A novel sensor to map auxin response and distribution at high spatio-temporal resolution. Nature *482*,103-106.

Burko, Y., Geva, Y., Cohen, R.A., Burko, S.S., Shani, E., Berger, Y., Halon, E., Chuck, G., Moshelion, M., and Ori, N. (2011). From organelle to organ: ZRIZI MATE-Type transporter is an organelle transporter that enhances organ initiation. Plant Cell Physiol *52*, 518-527.

Clough, S.J., and Bent, A.F. (1998). Floral dip: a simplified method for Agrobacterium-mediated transformation of *Arabidopsis thaliana*. Plant J *16*, 735-743.

Debeaujon, I., Peeters, A.J., Kloosterziel, L.M., and Koornneef, M. (2001). The TRANSPARENT TESTA12 gene of *Arabidopsis* encodes a multidrug secondary transporter-like protein required for flavonoid sequestration in vacuoles of the seed coat endothelium. Plant Cell *13*, 853-871.

Diener, A.C., Gaxiola, R.A., and Fink, G.R. (2001). *Arabidopsis* ALF5, a multidrug efflux transporter gene family member, confers resistance to toxins. Plant Cell *13*, 1625-1638.

Domagalska, M.A., and Leyser, O. (2011). Signal integration in the control of shoot branching. Biol Nat Rev Mol Cell *12*, 211-221.

Durrett, T.P., Gassmann, W., and Rogers, E.E. (2007). The FRD3-mediated efflux of citrate into the root vasculature is necessary for efficient iron translocation. Plant Physiol *144*, 197-205.

Ferguson, B.J., and Beveridge, C.A. (2009). Roles for auxin, cytokinin, and strigolactone in regulating shoot branching. Plant Physiol *149*, 1929-1944.

Hayward, A., Stirnberg, P., Beveridge, C., and Leyser, O. (2009). Interactions between Auxin and Strigolactone in Shoot Branching Control. Plant Physiol *151*, 400-412.

Kang, S.G., Jin, J.B., Piao, H.L., Pih, K.T., Jang, H.J., Lim, J.H., and Hwang, I. (1998). Molecular cloning of an Arabidopsis cDNA encoding a dynamin-like protein that is localized to plastids. Plant Mol Biol *38*, 437-447.

Lee, D.W., Kim, J.K., Lee, S., Choi, S., Kim, S., and Hwang, I. (2008). Arabidopsis nuclear-encoded plastid transit peptides contain multiple sequence subgroups with distinctive chloroplast-targeting sequence motifs. Plant Cell *20*, 1603-1622.

Lee, K.H., Kim, D.H., Lee, S.W., Kim, Z.H., and Hwang, I. (2003). In vivo import experiments in protoplasts reveal the importance of the overall context but not specific amino acid residues of the transit peptide during import into chloroplasts. Mol Cells *14*, 388-397.

Li. L., He, Z., Pandey, G.K., Tsuchiya, T., and Luan, S. (2002). Functional cloning and characterization of a plant efflux carrier for multidrug and heavy metal detoxification. Biol Chem *277*, 5360-5368.

Marinova, K., Pourcel, L., Weder, B., Schwarz, M., Barron, D., Routaboul, J.M., Debeaujon, I., and Klein, M. (2007). The Arabidopsis MATE transporter TT12

acts as a vacuolar flavonoid/H^+-antiporter active in proanthocyanidin-accumulating cells of the seed coat. Plant Cell *19*, 2023-2038.

Moriyama, Y., Hiasa, M., Matsumoto, T., and Omote, H. (2008). Multidrug and toxic compound extrusion (MATE)-type proteins as anchor transporters for the excretion of metabolic waste products and xenobiotics. Xenobiotica *38*, 1107-1118.

Müller, D., and Leyser, O. (2011). Auxin, cytokinin and the control of shoot branching. Ann Bot 107, 1203-1212.

Nawrath, C., Heck, S., Parinthawong, N., and Métraux, J.P. (2002). EDS5, an essential component of salicylic acid-dependent signaling for disease resistance in Arabidopsis, is a member of the MATE transporter family. Plant Cell *14*, 275-286.

Nguyen, H., Brown, R.C., and Lemmon, B.E. (2000). The specialized chalazal endosperm in Arabidopsis thaliana and Lepidium virginicum (Brassicaceae). Protoplasma *212*, 99-110.

Nordström, A., Tarkowski, P., Tarkowska, D., Norbaek, R., Astot, C., Dolezal, K,. and Sandberg, G. (2004). Auxin regulation of cytokinin biosynthesis in Arabidopsis thaliana: a factor of potential importance for auxin-cytokinin-regulated development. Proc Natl Acad Sci U S A *101*, 8039-8044.

Odell, J.T., Nagy, F., and Chua, N.H. (1985). Identification of DNA sequences required for activity of the cauliflower mosaic virus 35S promoter. Nature *313*, 810-812.

Omote, H., Hiasa, M., Matsumoto, T., Otsuka, M., and Moriyama, Y. (2006). The MATE proteins as fundamental transporters of metabolic and xenobiotic organic cations. Trends Pharmacol Sci *27*, 587-593.

Ongaro, V., and Leyser, O. (2008). Hormonal control of shoot branching. J Exp Bot *9*, 67-74.

Overvoorde, P.J., Okushima, Y., Alonso, J.M., Chan, A., Chang, C., Ecker, J.R., Hughes, B., Liu, A., Onodera, C., Quach, H., Smith, A., Yu, G., and Theologis, A. (2005). Functional Genomic Analysis of the AUXIN/INDOLE-3-ACETIC ACID Gene Family Members in Arabidopsis thaliana. Plant Cell. 17, 3282-3300.

Reed, J.W. (2001). Roles and activities of Aux/IAA proteins in Arabidopsis. Trends Plant Sci *17*, 420-425.

Rogg, L.E., Lasswell, J., and Bartel, B. (2001). A gain-of-function mutation in IAA28 suppresses lateral root development. The Plant Cell, *13*, 465-480.

Sambrook, J., Fritsch, E.F., and Maniatis, T. (1989). Molecular Cloning: a laboratory manual. C*old Spring Harbor Laboratory Press* ISBN 0-87969-309-6, 1659.

Sessions, A., Weigel, D., and Yanofsky, M.F. (1999). The Arabidopsis thaliana MERISTEM LAYER 1 promoter specifies epidermal expression in meristems and young primordia. Plant J *20*, 259-263.

Seo, P.J., Park, J., Park, M.J., Kim, Y.S., Kim, S.G., Jung, J.H., and Park, C.M. (2012). A Golgi-localized MATE transporter mediates iron homoeostasis under osmotic stress in Arabidopsis. Biol Chem *442*, 551-561.

Sun, X., Gilroy, E.M., Chini, A., Nurmberg, P.L., Hein, I., Lacomme, C., Birch, P.R., Hussain, A., Yun, B.W., and Loake, G.J. (2011). ADS1 encodes a MATE-transporter that negatively regulates plant disease resistance. New Phytol *192*, 471-482.

Tanaka, M., Takei, K., Kojima, M., Sakakibara, H., and Mori, H. (2006). Auxin controls local cytokinin biosynthesis in the nodal stem in apical dominance. Plant J *45*, 1028-1036

Thompson, E.P., Wilkins, C., Demidchik, V., Davies, J.M., and Glover, B.J. (2010). An Arabidopsis flavonoid transporter is required for anther dehiscence and pollen development. Exp Bot *61*, 439-451.

Thompson, E.P., Davies, J.M., and Glover, B.J. (2010). Identifying the transporters of different flavonoids in plants. Plant Signal Behav *5*, 860-863.

Weigel, D., Ahn, J.H., Blazquez, M.A., Borevitz, J.O., Christensen, S.K., Fankhauser, C., Ferrandiz, C., Kardailsky, I., Malancharuvil, E.J., and Neff, M.M. (2000). Activation tagging in Arabidopsis. Plant Physiol *122*, 1003 -1013.

Zhao, J., and Dixon, R.A. (2009). MATE transporters facilitate vacuolar uptake of epicatechin 3'-O-glucoside for proanthocyanidin biosynthesis in Medicago truncatula and Arabidopsis. Plant Cell *21*, 2323-2340.

국문 초록

ATL98246 돌연변이는 애기장대 Columbia ecotype (Col-0)의 활성화표지 돌연변이주에서 다지형 표현형을 보여 선별하였다. *ATL98246* 돌연변이는 장일 조건에서 정단우성이 약해진 bushy dwarf 표현형으로 보인다. Plasmid rescue 를 통하여 *ATL98246* 돌연변이의 T-DNA 삽입 위치를 결정한 결과 *At5g19710* 유전자의 단백질 암호화 부위에 삽입되어 있음이 밝혀졌다. RT-PCR 결과 T-DNA 의 *CaMV 35S* enhancer에 의해 *At5g19700* 유전자의 발현이 증가되었음을 확인하였다. *CaMV 35S* 프로모터를 이용한 recapitulation 실험을 통해 *At5g19700* 유전자의 과발현에 의해 다지형 표현형이 나타남을 확인할 수 있었다. *At5g19700* 유전자는 multidrug and toxic compound extrusion (MATE) transporter 의 단백질을 암호화하고 있다. *GUS* 돌연변이체와 RT-PCR을 통해 유전자의 발현을 확인한 결과 어린 잎, 떡잎의 관다발, 뿌리의 관다발, 화서 그리고 종자에서 발현함이 확인되었다. *ATL98246* 돌연변이에서 auxin 의 변화되어 다지형 표현형이 나타남을 예상할 수 있다.

ACKNOWLEDGEMENT

First and foremost, I would like to thank to my supervisor, Dr. Lee Jong Seob for his support during my two and a half years master course study. He gave me a lot of guidance and advice in my study and research. Also, I would like to thank to the other committee members, Dr. Cho Hyung Taeg and Dr. Lee Ji Young. I am very grateful for their probing questions and critical comments of my study.

Thank to the other members in our lab, Jeong Cheol Woong, Roh Hyung Min and Lee Sook Jin. They provided me with valuable guidance in my study, experiment and writing of this thesis with impressive kindness and patience. Without their instruction, I could not have completed my master degree. I also thank Jin Yin Hua. She helped me a lot in both my study and my life when I came Korea alone two years ago.

Most importantly, I want thank my family even though they were not in my side. As the single daughter in my family, I know how hard for you to be apart with me. Thank you for consistently encouraging me to be brave, independent and optimistic. And my friends, with whom I shared my happiness and pain, gave me much encouragement and support when I was in the hard times. Thank you very much.

Yao Jingyi

Seoul/2012.01.02